Grid Code Testing of Full Power Converter Based Wind Turbines Using Back-to-Back Voltage Source Converter System

Nicolás Espinoza, Massimo Bongiorno and Ola Carlson.
Chalmers University of Technology, Energi och Miljö, Elteknik.
Hörsalsvägen 11, 412 96 Gothenburg, Sweden.
nicolas.espinoza@chalmers.se, Tel.: +46 31 772 1650.

Summary

This paper presents an alternative approach of grid code testing for wind turbines (WTs) using back-to-back Voltage Source Converter (VSC). In particular, this paper focuses on grid code analysis for WTs, and low voltage ride through (LVRT) testing for full power converter (FPC) based WTs. Recent European grid codes are analyzed and selected for testing according to their strictness and wind power penetration in each country. The investigated testing setup consists of a 4 MW FPC-based WT and an 8 MW back-to-back VSC system, operated as a test equipment. The effectiveness of the investigated grid code testing method is validated using the simulation tool PSCAD/EMTDC, where the electrical systems of the WT as well as the test equipment are modeled in detail. A control strategy for the WT is given; in addition, hardware and control algorithms for the converter-based test equipment are described, with special focus on their limitations for testing procedures. The results demonstrate the capability of the investigated testing device in producing a controllable voltage dip at the terminals of the WT, at the same time that is being fed with short circuit currents. Moreover, its flexibility in emulating the behavior of the grid in continuous and dynamic condition is highlighted and discussed in extent.

Introduction

In countries where wind power has become a relevant part of the total generated electrical power production, transmission system operators (TSOs) have included in their grid codes specific technical requirements for interconnection of wind parks. Disregarding topologies and geographical location, grid codes state how wind parks should behave under both continuous and dynamic conditions while maintaining a safe and reliable operation.

On-site test verification of grid code compliance is today performed by using, for example, a set of impedances to control the amplitude and phase of the applied voltage at the terminals of the WT [19]. However, the quantity of case studies achievable with this testing device is limited given the restricted combination of realizable voltages; furthermore, other kinds of disturbances, for example frequency deviations, remain unverified. Moreover, a more comprehensive methodology of grid code testing is recommended due to the exhaustive technical requirements that today's TSOs impose on WT manufacturers. For example the variety of control actions for active and reactive power during frequency deviation or during voltage dips, especially for voltage recovery ramps, among different grid codes. The use of back-to-back VSC system as a test equipment addresses this issue in an efficient way, thanks to its controllability and versatility.

This paper contains studies regarding interconnection of WTs and it presents an alternative approach of grid code testing by using VSC-based testing equipment. Selected grid codes from different European countries are analyzed. Technical requirements regarding active and reactive power management for different voltage and frequency operation ranges are described and compared. The electrical model presented in this paper resembles an actual setup: the "Big Glenn" WT, constituted by a 4 MW FPC-based WT and a high voltage 9 MW back-to-back converter system, which was recently installed for testing purposes in Gothenburg, Sweden [16]. The given control strategy of the test equipment allow to replicate grid dynamic behavior at the terminals of the WT. Two representative voltage dips are applied at different power production levels of the WT, showing the flexibility of the use of VSC for grid code testing. Finally, the results shown that by using a VSC-based testing equipment, a more reliable representation of grid dynamic conditions can be achieved.

Grid Code Selection

The selected grid codes refer to countries that present a high penetration of wind power in their national grid. Consequently, these countries have developed detailed technical requirements for interconnection of wind power plants.

The following grid codes were chosen given its detailed section regarding interconnection of wind farm with the electricity grid, with focus on voltage and frequency operation band, voltage and reactive power dependencies, active power curtailment and low voltage ride through requirements. The selected grid codes are: the German (E.ON) [5] and [6]; British (National Grid) [7]; Spanish (REE) [8]; Irish (EirGrid) [9]; Danish (Energinet.dk) [10], Swedish (Svenska Kraftnät) [11]; Nordic Countries (Nordel) [12]; and European grid code (ENTSO-E) [13]. Moreover, wind power penetration data can be found in [14]. Comparison of the different grid codes regarding interconnection of WTs is given in [1] to [4]. Finally, control strategies meeting grid code technical requirements have been documented in [15].

Voltage and frequency deviation in continuous operation

In grid codes, it is specified the steady state frequency and voltage operation range in which the WT should operate in continuously. Normal condition is considered for voltages close to 1.0 pu and frequency around 50 Hz, with deviation of ±0.05 pu of voltage and ±0.5 Hz of frequency. Any grid condition outside these values is defined with a minimum operational time, and in some cases, followed by a control action for active or reactive power from the WT side. A well-documented explanation of voltage-frequency restrictions is given in [1] and [2], and in each grid codes from [5] to [11].

The strictest requirement among the selected grid codes in terms of operation during frequency deviation is imposed by the German TSO E.ON to offshore WTs [5], which stipulates that the WT should stay connected during minimum 3 seconds when the grid frequency is in the range of 46.5 Hz to 47.5 Hz and 51.5 Hz to 53 Hz. During intermedium frequency ranges away from nominal frequency, the German grid code defines intervals from 10 second to 30 minutes of operation [2], [5], [6]. Regarding voltage deviation, the Danish grid code [10] rigorously imposes continuous operation for voltages from 0.09 pu to 1.1 pu, within a frequency range of 49.5 Hz to 50.2 Hz.

Without considering a wide voltage range, another strict requirement is given by the British grid code [7], which states that WTs should remain connected in continuous operation when the grid frequency is in the range of 47.5 Hz to 52 Hz. In this case, the voltage range is from 0.95 pu to 1.05 pu for the 400 kV system.

Active Power Curtailment

When active power curtailment is allowed in case of frequency deviations, the generation unit must change its active power output in order to contribute to the overall regulation of the system frequency.

A well-documented strategy for frequency control is given in the Irish grid code, as shown in Figure 1(a). A normal frequency range is defined between the point “B” and “C”, where no frequency variation is compensated. If the frequency drops from the defined dead band, the wind farm should respond according to the segment “AB”. Similarly, when the frequency rises above the dead band, active power production is varied according to segment “CD”. Interruption of active power production is required when frequency raises the unique frequency where the segment “DE” is defined.

A similar control strategy for frequency response is given by the Danish authority, as depicted in Figure 1(b). Values for “fmin” and “fmax” are settled according to the frequency operation range of the wind farm. The frequencies “f2” and “f3” define the dead band, where the active power production remains unchanged when frequency variation occurs. Moreover, the control band is defined between the frequencies “f1” and “f4”, where a dedicated frequency control operates by varying the active power production. Similarly to the Iris grid code, “Droop 1” and “Droop 2” have similar purposes of segments “AB” and “CD” respectively. Finally, “Droop 3” and “Droop 4” define a curve in which the wind farm has to provide critical power-frequency control when needed.

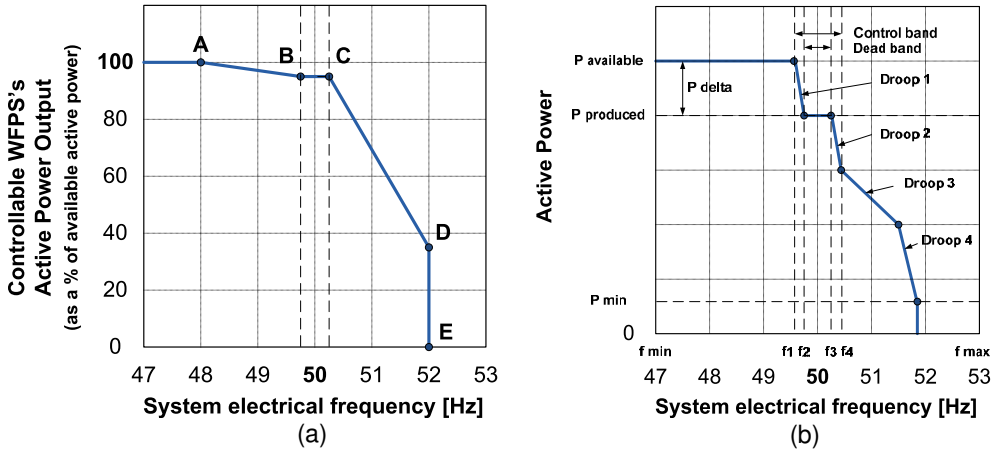

Figure 1 Power-frequency curve according to the (a) Irish [9], and (b) Danish [10] grid codes.

A requirement for active power curtailment is also given by the German grid code [6]. A droop control is suggested for frequencies above 50.2 Hz. Disconnection within 300 ms of the whole wind park is allowed when frequency rises over 53.5 Hz or when it drops under 46.5 Hz. In addition, requirement for varying the active power production is restricted by a given ramp rate that the wind park has to track. The German grid code, for instance, stipulates a gradient of 40% of the available active power per Hz deviation when frequency exceeds 50.2 Hz.

More specifications about active power curtailment can be found among any grid code, and it is also explained in [1] to [4].

Reactive power requirements during normal operation

A TSO can also require reactive power injection from the wind farms to support overall system voltage control during normal operation. Usually, reactive power requirements are delimited inside a minimum power factor range that goes from 0.95 leading to 0.95 lagging, which is equivalent to ±0.33 pu of reactive power; and within a nominal voltage that varies with a maximum deviation of ± 0.05 pu.

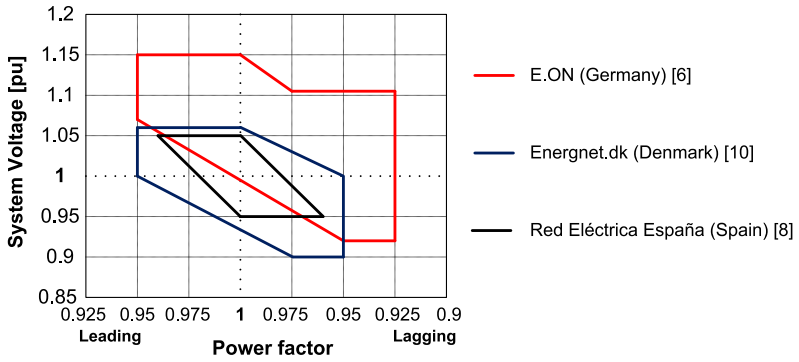

Figure 2 Example of normalized voltage-reactive power dependencies among the selected grid codes.

A normalized comparison of dependencies among different grid codes is shown Figure 2. A non-strict dependency is enforced by the Spanish grid code for the 400 kV system. On the contrary, an example of a strict reactive power constrain is given in the German grid code, in which the maximum voltage to withstand is above 1.15 pu in the 380 kV system.

Reactive power requirement are also dependent of the active power production of the wind farm. The Danish grid code states dependencies between voltage and reactive power, and between active and reactive power production. Both requirements shall be complied simultaneously during normal operation of the wind farm. The Irish grid code [9] enforces a particular requirement

defining a constant ratio between active and reactive power when the active power production is within the range of 0.5 pu to 1 pu. When active power drops below the previous range, the wind farm has to be able to operate with a power factor from 0.835 leading to 0.835 lagging. Additionally, after a step change in the voltage reference, 90% of the new steady state reactive power set point must be reached within one second.

As previously explained, reactive power injection can be controlled by either using a voltage control or power factor control. An extra option to define a reactive power production set point is to manually control the operation point. Remote control of reactive power allows TSO to control the voltage at a distance node, and in general, to control the total reactive power production of an entire grid. Finally, when meeting grid code requirement, FACTS technologies such as STATCOM or SVC are used to enhance reactive power capabilities of a wind farm. This concept has been analyzed, for instance, in [15].

Low voltage ride through (LVRT)

In every grid code, it is specified a voltage dip profile that the WT should ride through without tripping. An exhaustive comparison of LVRT profiles is given in [1]. LVRT profiles characterization in terms of fault time, retained voltage and recovery ramp rates can be found in [3]. In Figure 3 is shown a combination of the strictest LVRT profiles among the selected grid codes. A generic waveform of a LVRT profile and voltage dip is also depicted in Figure 4. The European grid code [13] defines the guidelines to establish the LVRT profiles in each network inside EU. The requirements enforced by ENTSO-E are not as strict as the local requirements, since they basically cover a wide voltage and time ranges.

When it is specified in the grid code, WT are required to support voltage restoration by injecting reactive power into the grid [1] to [4]. The generating plant must provide voltage support with an additional reactive power injection during a voltage dip. For example, the Danish grid code [10] enforces a specific LVRT with retained voltage of 0.2 pu per 500 ms, and demands for reactive power support during voltage restoration. Reactive current must be injected when voltage deviates below 0.9 pu. When the system voltage is lower than 0.5 pu, nominal reactive current must be reached. Active power production must be restored within 5 seconds after full recovery of the voltage within normal operation range.

According to the German grid code [6], an automatic voltage control must be activated within 20 ms if the grid voltage deviates more than 0.1 pu, and it must inject at least a current of 0.02 pu for each percent of voltage deviation. For off-shore wind farms [5], the voltage control must be activated when grid voltage deviates 0.05 pu from its nominal value. Full reactive power output must be achieved when voltage drops more than 0.5 pu, similarly to the Danish grid code. After fault clearance, the automatic voltage control must still be active for another 500 ms after returning of the voltage within the normal operation band, in order to compensate for any voltage variation due to a second failure in the system. Finally, the pre-fault set point of active power production must be reached with a gradient of at least 0.2 pu per second after returning of the voltage within the normal operation range.

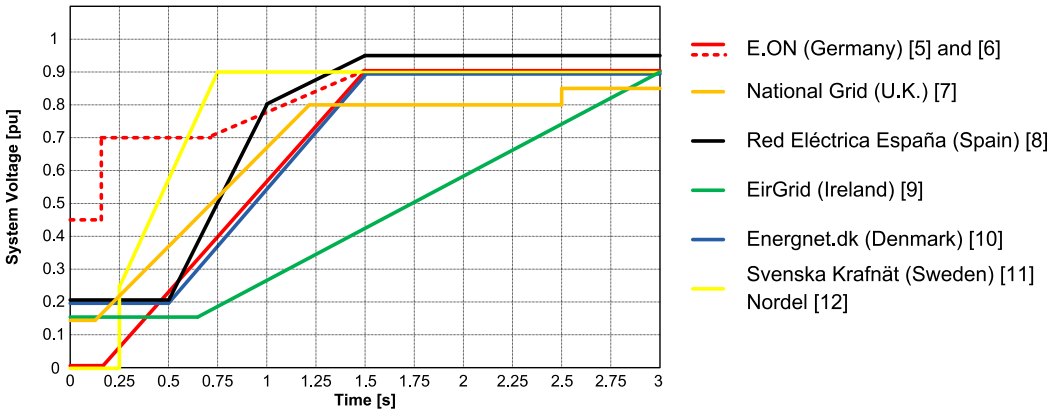

Figure 3 Example of LVRT profiles from the selected grid codes.

A strict LVRT profile is defined in the Irish grid code, which enforces a minimum retained voltage of 0.15 pu for 650 ms, followed by a voltage recovery ramp for 3 seconds. During the voltage dip, the wind farm shall provide active power in proportion to retained voltage while maximizing reactive current injection into the grid, for at least 600 ms or until the voltage recovers to within its normal operational range. In addition, the wind farm must be able to reach 90% of its available active power production within one second, after a total voltage recovery. The Irish grid code enforces reactive current injection of 0.04 pu, per each percentage of voltage drop when this is lower than 0.9 pu. Maximum power should be injected when the voltage drops below 0.75 pu [3].

The Swedish grid code defines a retained voltage value of 0 pu for 250 ms, followed by voltage a ramp up to 0.9 pu for one second. The reactive power exchanged between the WT and the power system is strictly defined in 0 pu for the whole event [11].

Modeling of the Wind Turbine and Test Equipment

System overview

A complete overview of the test system is shown in Figure 4 [16]. The FPC-based WT is modeled by using a synchronous generator connected to a VSC in back-to-back configuration, with a step-up transformer in its output. The test equipment is constituted by two VSC connected in back-to-back, doubling the power rating of the WT. The generated power flows from the generator through the FPC and finally it is injected via output transformer into the collector side (PCC) of the test equipment.

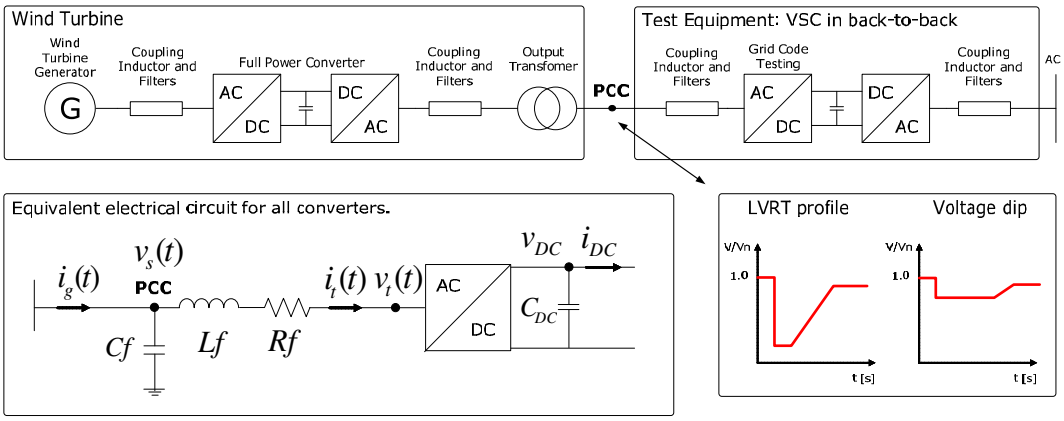

Figure 4 Test setup overview and equivalent circuit.

Power and voltage rating of the testing setup

System parameters of the WT and test equipment are given in Table 1.

Table 1 System parameters for the WT and test equipment.

	Wind Turbine	**Test Equipment**
Type	FPC-based	VSC Back-to-back
Power	4.1 MW	9 MVA
RMS Voltage	690 V	10.5 kV
RMS Current	3350 A	500 A
Output Transformer	4.6 MVA; 0.690/10.5 kV	

Control overview

The overview of the utilized cascade-controller for all converters is shown in Figure 5. The reference currents for the inner current controller are generated by three different outer controllers: active power control or DC voltage control, and reactive power control. Each converter utilizes a specific control mode in order to generate the dedicated current references. The inner current controller calculates the reference output voltage of the converter. The three-phase normalized reference output voltages are then sent to the pulse width modulator control to generate the gate signals of the converter.

In the FPC, the generator-side converter is controlling the active power entering into the DC-link, while the grid-side converter is controlling the DC-link voltage by exchanging active power at the low voltage-side of the output transformer. A dedicated reactive power control is also implemented in this converter. The step-up transformer is directly connected to the collector side of the test equipment. The PCC converter of the test equipment controls the AC voltage at the terminals of the WT, while the grid-side converter is connected to a stiff AC grid maintaining the DC-link voltage stable.

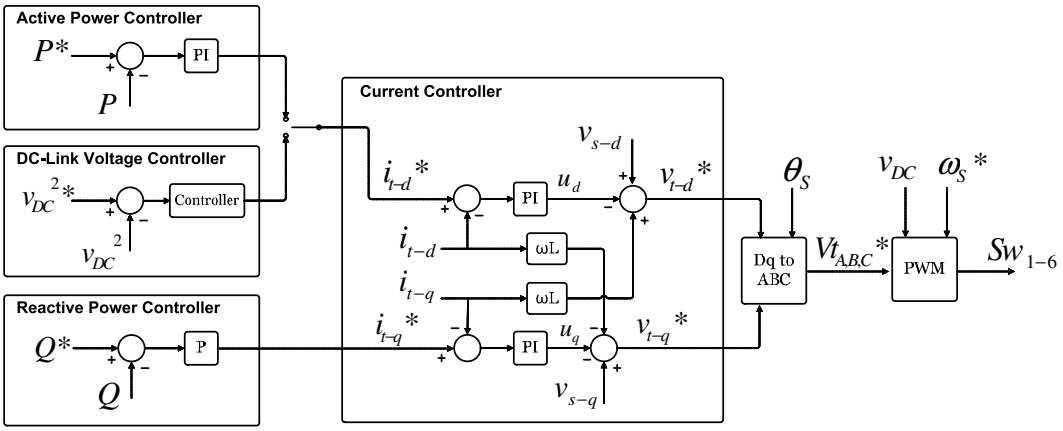

Figure 5 Control Overview

Phase locked loop

The implemented phase locked loop (PLL) is shown in Figure 6. The quadrature component of the system voltage v_{s-q} is tracked and controlled in zero by using a PI controller. The output signal of the PI controller $\partial\omega_S$ is added to the reference angular frequency ω_S^*. The total frequency signal includes the reference and the control signal to maintain Vs_q in zero, and it is integrated to obtain the transformation angle θ_S. Moreover, this particular voltage alignment implemented in the PLL allows to separate the total current vector $\underline{i}^{(dq)}$ in two components: the direct axis component i_d, in phase with the system voltage, which represent the active current in steady state; and the quadrature axis component i_q which in steady state correspond to the reactive current. More information about the implemented PLL is given in [21].

Clark's and Park's transformation

A Clark's and Park's transformation block schemes are shown in Figure 6. The system voltage is composed by three phase to ground instantaneous voltages: $\underline{v}_s(t) = \{v_{s-a}(t), v_{s-b}(t), v_{s-c}(t)\}$. Similarly, the current signal measured at the terminals of the converter encloses three instantaneous line currents: $\underline{i}_t(t) = \{i_{t-a}(t), i_{t-b}(t), i_{t-c}(t)\}$. Via reference frame transformation of the three-phase vectors using the transformation angle θ_S from the PLL block, it is possible to obtain the direct and quadrature axis component of the system voltage vector in dq frame $\underline{v}_s^{(dq)}$, and line current vector in dq frame $\underline{i}_t^{(dq)}$: the pair v_{s-d} and v_{s-q}, and the pair i_{t-d} and i_{t-q} respectively. By using the same procedure, the grid three-phase current vector $\underline{i}_g(t)$ is transformed into $\underline{i}_g^{(dq)}$, composed by the pair i_{g-d} and i_{g-q} existing in the Park's rotating frame.

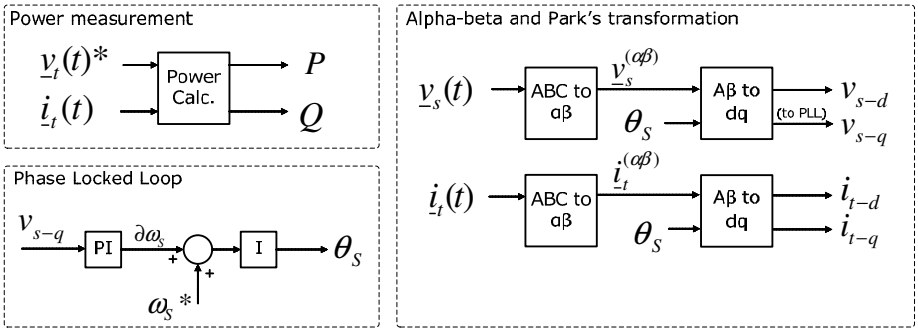

Figure 6 Implemented measurement block.

Current control

The implemented decoupled current control is shown in Figure 5. The dynamics of the instantaneous current $\underline{i}_t(t)$ between the PCC and the terminals of the converter can be obtained from the following transformed equations:

$$\frac{di_{t-d}}{dt}L_f + i_{t-d}R_f - \omega_s L_f i_{t-q} = v_{s-d} - v_{t-d} \tag{1}$$

$$\frac{di_{t-q}}{dt}L_f + i_{t-q}R_f + \omega_s L_f i_{t-d} = v_{s-q} - v_{t-q} \tag{2}$$

The coupling terms $\omega_s L_f i_{t-d}$ and $\omega_s L_f i_{t-q}$ must be cancelled in steady state when devising the current control loop. The current control strategy in Laplace form can be expressed as follows:

$$\underline{\varepsilon_{rr}}_{It}^{(dq)}(s) = \underline{i}_t^{(dq)^*} - \underline{i}_t^{(dq)} \tag{3}$$

$$\underline{v}_t^{(dq)^*}(s) = \underline{v}_s^{(dq)} - j\omega_s L_f \underline{i}_t^{(dq)} - \left(k_p + \frac{k_i}{s}\right)\underline{\varepsilon_{rr}}_{It}^{(dq)}(s) \tag{4}$$

As a result, the control action u_d and u_q shown in Figure 5 controls independently the direct and quadrature axis component of the terminal current, i_{t-d} and i_{t-q} respectively. The methodology for deriving the current control is given in [18].

DC voltage control for back-to-back converter

The implemented DC voltage control strategy in Laplace form is written in (5) and (6):

$$\varepsilon_{rr\,DC}(s) = {v_{DC}^*}^2 - {v_{DC}}^2 \tag{5}$$

$$i_{t-d}^*(s) = \left(k_p + \frac{k_i}{s}\right)\varepsilon_{rr\,DC}(s) + k_p {v_{DC}}^2 + \frac{2}{3}\frac{i_{DC}v_{DC}}{\widehat{V_{base}}} \tag{6}$$

where $i_{t-d}^*(s)$ is the current reference that controls the DC Voltage. Active damping is also introduced in the controller by feedforward of the transmitted DC power. More information of the proposed control is found in [20] and [21].

AC voltage control in collector side of Test Equipment

A dedicated voltage control with no PLL has been used to control the voltage at the terminals of the WT. By this means, it is possible to control the applied voltage in terms of magnitude, frequency and phase angle. The reference voltage is defined by the equivalence

$$\underline{v}_s^{(dq)^*} = V_s \angle \delta_S \tag{7}$$

The magnitude V_s and the phase angle δ_S are manually selected. The frequency is easily calculated by integration of the angular frequency reference ω_S^*, neglecting the action of the PI controller shown in Figure 6. The calculated instantaneous position θ_S and the resulting voltage vector $\underline{v}_s^{(dq)^*}$ are feed into the voltage controller.

The given AC voltage control strategy in Laplace form is written as follows:

$$\underline{\varepsilon_{rr}}_{Vs}^{(dq)}(s) = \underline{v_s}^{(dq)^*} - \underline{v_s}^{(dq)} \tag{8}$$

$$\underline{i_t}^{(dq)^*}(s) = \left(\frac{\alpha_f}{s+\alpha_f}\right)\underline{i_g}^{(dq)^*} + j\omega C_f \underline{v_s}^{(dq)} + \left(k_p + \frac{k_i}{s}\right)\underline{\varepsilon_{rr}}_{Vs}^{(dq)}(s) \tag{9}$$

Additional information of the implemented voltage control, including PI controller gains and low pass filter bandwidth is given in reference [17].

Grid Code Testing

Voltage dip

A symmetrical voltage dip is applied at the terminals of the WT (HV side of the WT output transformer, denoted as PCC in Figure 4). The applied voltage is controlled in 1 pu and it is reduced with a step function to 0.7 pu at t = 0.5 seconds. The voltage is retained for 1 second and restored with a ramp function to its pre-fault value. The WT is producing half of its nominal active power which corresponds to a power of 0.25 pu in the test equipment base system, according to Table 1. The voltage, the output current and output active and reactive power of the WT are measured at the PCC. The current $\underline{i_t}(t)$ at the terminals of the test equipment shown in Figure 5 is also measured. The results are shown in Figure 7.

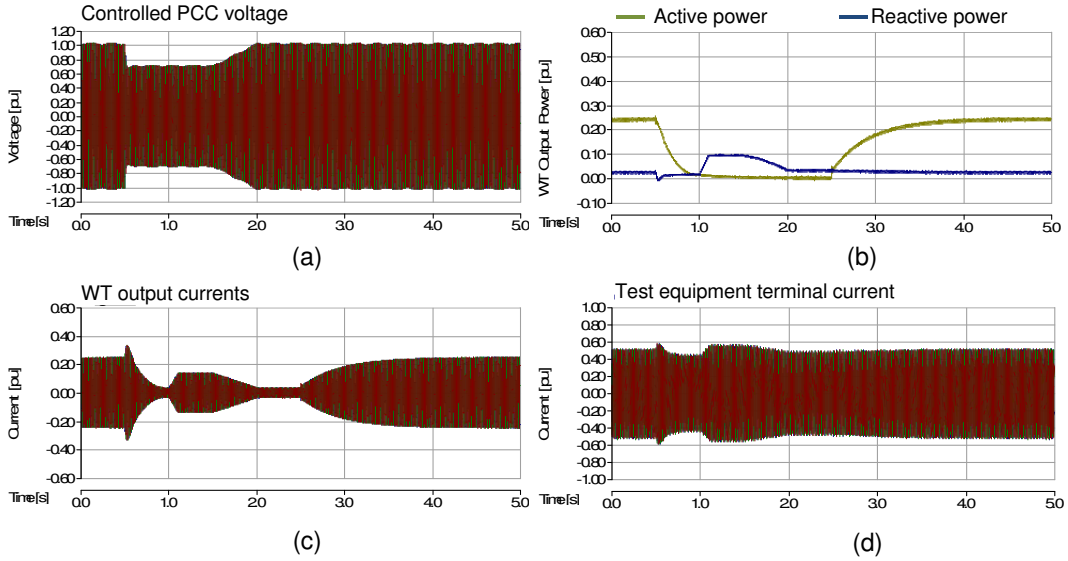

Figure 7 Voltage dip 0.7 pu. (a) Controlled PCC voltage, (b) WT output power, (c) WT output currents, and (d) test equipment terminal current.

The WT reduces its output power within 500 ms after recognition of the voltage dip. The output current rises given the long time constant of the power control and the reduced voltage at the PCC. Reactive current is being injected to the PCC in t = 1 second rising up the reactive power to 0.1 pu. The voltage is fully restored in t = 2.5 seconds and the WT starts to produce active power 500 ms after, reaching its pre-fault value at t = 4.5 seconds. Finally, the terminal current of the test equipment follows the shape of the output current of the WT, but with the addition of the VSC filter current, reaching a maximum of 0.6 pu.

Symmetrical LVRT test

This test is performed by applying at the PCC the LVRT profile given in the Danish grid code [10], also depicted in Figure 3. The voltage is reduced to 0.2 pu for 500 ms, and restored to 0.9 within the next 1 second. In this scenario, the WT is producing nominal active power. The measurement points are kept unchanged. The results are shown in Figure 8.

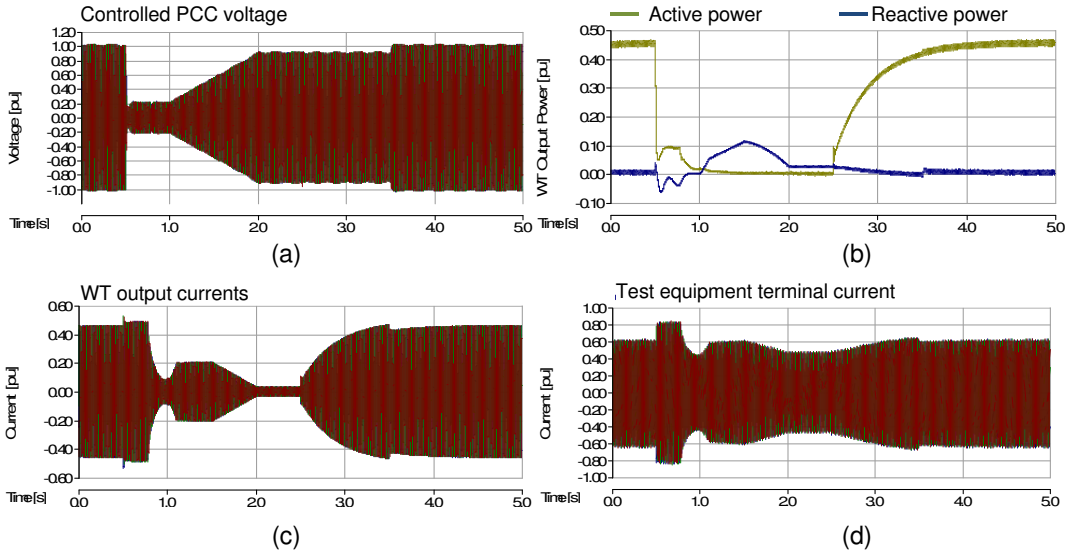

Figure 8 LVRT test. (a) Controlled PCC voltage, (b) WT output power, (c) WT output currents, and (d) test equipment terminal current.

When the PCC voltage is abruptly reduced, the WT reduces its output power much faster than the previous case. The activation of the DC crowbar at the FPC redirect the excess of energy injected to the DC-link into an internal resistor. In addition, during the whole voltage dip the FPC reaches current limitation, injecting 0.5 pu current at the PCC. With the addition of the filter current, the terminal current of the test equipment reaches 0.82 pu. Full reactive current is being injected during the recovery of the PCC voltage. However, the total reactive power is limited to a maximum of 0.13 pu due to the low voltage retained PCC. The reactive current is gradually reduced when the voltage is reaching 0.9 pu. Finally, the WT starts to produce active power after 500 ms of full recovery of the voltage within the normal operation band, reaching its nominal production at t = 5 seconds.

Conclusions

In the first part of this paper it is given a comparison of grid codes from European countries regarding interconnection of WT. Dependencies between system voltage, grid frequency, and reactive power production are discussed in extent. Moreover, active power control strategies against frequency deviation are also illustrated and explained. Finally, LVRT profiles are compared in terms of strictness and reactive power management during the voltage dip.

The second part focuses in a different approach of grid code testing of WT. The investigated testing device and its given control strategy is used to replicate the grid behavior at the terminals of the WT. The reliability of the test equipment is verified by simulation. The ability of the converter in producing voltage drops is illustrated in two representative case studies in which the WT is set at different operating point.

Future Work

The simulation model presented in this paper will be validated with experimental results by using a laboratory setup constituted by a 150 kW synchronous generator, connected to a 100 kW VSC in back-to-back representing the FPC-based WT, and a second 100 kW back-to-back converter operated as a test equipment, as described in this work. Finally, field test of the 4 MW GE WT “Big Glenn” by using the 8 MW ABB HVDC-Light is programmed for autumn 2013, giving a unique opportunity of testing, for example, voltage dips at different frequencies.

Acknowledgements

The authors would like to acknowledge Swedish Energy Agency and Swedish Wind Power Technology Centre their aid with funding; and the authors would also like to acknowledge ABB, General Electric and Göteborg Energi for their aid with funding and for providing data used in the models.

References

1. M. Tsiliand and S. Papathanassiou, “A review of grid code technical requirements for wind farms”, IET Renewable Power Generation. September 2009; 3:308-332.
2. M. Altin, O. Goksu, R. Teodorescu, P. Rodriguez, B.K. Jensen and L. Helle, “Overview of recent grid codes for wind power integration”. Proceedings to the 12th international conference OPTIM 2010.
3. M. Mohseni and S.M. Islam, “Review of international grid code for wind power integration: Diversity, technology and a case for global standard”. Renewable and Sustainable Energy Reviews, Romania, 2012; 16:3876-3890.
4. I. Erlich and U. Bachmann, “Grid code requirements concerning connection and operation of wind turbines in Germany”. Power Engineering Society General Meeting. June 2005; 2:1253-1257.
5. E.ON Nets. Requirements for Offshore Grid Connection in the E.On Nets Network. April 1st, 2008.
6. E.ON Nets GmbH, Baireuth. Grid Code – High and extra high voltage. Status: April 1st 2006.
7. National Grid Electricity Transmission plc. The grid code. Issue 4, Revision 13, June 7th, 2012.
8. Red Eléctrica España. P.O.12.3 Requisitos de respuesta frente a huecos de tensión de las instalaciones de producción de régimen especial. Resolución de 04-10-2006, BOE October 24th, 2006.
9. EirGrid. EirGrid Grid Code Version 4.0. December 8th, 2012.
10. Energinet.dk. Technical regulation 3.2.5 for wind power plants with a power output greater than 11 kW. Rev 4.1. September 30th, 2010.
11. Svenska Krafnät. Affärsverket svenska kraftnäts författningssamling SvKFS 2005:2. December 9th, 2005.
12. Nordel. Nordic Grid Code 2007(Nordic collection of rules). 15th January 2007.
13. Europe, ENTSO-E Network Code for Requirements for Grid Connection Applicable to all Generators. June 26th, 2012.
14. WWEA, World Wind Energy Report 2010; June 2011. Available at: http:www.wwindea.org.
15. M. Molinas, J.A. Suul, and T. Undeland. “Simple Method for Analytical Evaluation of LVRT in Wind Energy for Induction Generators with STATCOM or SVC”. SINTEF Energy Research, Trondheim, Norway, 2007.
16. Göteborg Wind Lab. Available at www.goteborgwindlab.se.
17. M. Bongiorno and A. Petterson. Development of a Method for Evaluation of Wind Turbines Ability to Fulful Swedish Grid Codes. Elforsk rapport 09:25. February 2009.
18. L. Harnefors and H-P Nee. “Model-Based Current Control of AC Machines Using the Internal Model Control Method”. IEEE Trans. Ind. Appl., January/February 1998; 34,2:133-141.
19. I. Martinez and D. Navarro. “Gamesa DAC converter: the way for REE grid code certification”. 13th International Power Electronics and Motion Control Conference. September 2008; 437-443.
20. R. Ottersten, “On control of back-to-back converters and sensorless induction machine drives” Ph.D. dissertation, Chalmers Univ. of Technol., Göteborg, Sweden, June 2003.
21. M. Bongiorno and T. Thiringer. “A Generic DFIG Model for Voltage Dip Ride-Through Analysis”. IEEE Trans. On Energy Conversion. January 2013; 99:1-10.